CHEMISTRY

Cooperative chemoenzymatic synthesis of N-heterocycles via synergizing bio- with organocatalysis

Zhuotao Tan[1,2], Xiaowang Zhang[1], Mengjiao Xu[1], Yaping Fu[1], Wei Zhuang[1], Ming Li[1], Xiaojin Wu[3], Hanjie Ying[1,2], Pingkai Ouyang[1,2], Chenjie Zhu[1,2]*

Inspired by Nature's ingenuity, considerable progress has been made in recent years to develop chemoenzymatic processes by the integration of environmentally friendly feature of biocatalysis with versatile reactivity of chemocatalysis. However, the current types of chemoenzymatic processes are relatively few and mostly rely on metal catalysts. Here, we report a previously unexplored cooperative chemoenzymatic system for the synthesis of N-heterocycles. Starting from alcohols and amines, benzimidazole, pyrazine, quinazoline, indole, and quinoline can be obtained in excellent yields in water with O_2 as the terminal oxidant. Synthetic bridged flavin analog is served as a bifunctional organocatalyst for the regeneration of cofactor nicotinamide adenine dinucleotide in the bioprocess and oxidative cyclodehydrogenation in the chemoprocess. Compared to the classical acceptorless dehydrogenative coupling strategy, being metal and base free, requiring only water as solvent, and not needing atmosphere protection were observed for the present method, exhibiting a favorable green and sustainable alternative.

INTRODUCTION

Nature metabolism networks have conferred the ability to synthesize diverse biomolecules and other metabolites that support life, which are attributed to the multistep cascade reactions catalyzed by mutually compatible and selective enzymes in living organisms. Inspired by these biological cascade systems (*1*–*3*), chemoenzymatic cascade processes by the integration of environmentally friendly feature of biocatalysis with versatile reactivity of chemocatalysis have recently drawn considerable attention (*4*). As a result of its simplified operation (omitting the isolation and purification of intermediates), lower cost, enhanced selectivity, less waste generation, and higher overall yields, chemoenzymatic process is nowadays a popular strategy for fine chemical synthesis (*5*–*7*). According to the classification proposed by Zhao and colleagues (*8*), there are three types of chemoenzymatic process, namely, sequential, concurrent, and cooperative chemoenzymatic reactions (CCRs). Among these three types, CCRs have shown great advantages because they could generate products in yields and/or selectivities higher than those obtained from the sequential reactions of the individual biocatalysts or chemocatalysts on their respective substrates. Until now, the vast majority of reported CCR could be divided into only two categories: One is chemocatalyst-catalyzed reversible reaction followed by irreversible enzymatic reaction, represented by dynamic kinetic resolution (DKR) of racemic amines or alcohols (Fig. 1A) (*9*). In the other case, chemocatalyst is only served for cofactor regeneration in enzymatic reaction (Fig. 1B) (*10*). The reported chemocatalysts for CCR acted only on the part of the chemoprocess or cofactor regeneration, and metal complexes are the most commonly used for this purpose (*11*, *12*). However, mutual inactivation of the metal catalyst and enzyme is often observed because of the undesirable bonding between the metal complex and nucleophilic residues of enzyme (*13*–*15*). The example of chemocatalyst acting as a bifunctional catalyst that plays dual roles in both bio- and chemoprocess has not been reported so far to the best of our knowledge (Fig. 1C). In these contexts, the development of new chemoenzymatic reaction type and nonmetallic catalyst for expanding the scope of CCR is highly attractive.

N-heterocyclic compounds, as an important framework, feature widely in pharmaceuticals, dyes, agrochemicals, and functional materials (*16*–*19*). The widespread interest in these privileged scaffolds has promoted extensive studies on their synthesis. The straightforward methods include the heterocyclization of amine with either carboxylic acids/derivatives (nitriles, orthoesters, and imidates) (*20*, *21*) or aldehyde (*22*). The other method is intramolecular oxidative cyclization of aniline Schiff base, which is often generated in situ from the condensation of amine and aldehyde. An alternative atom-economical and environmentally friendly approach for the synthesis of these compounds is one-pot multistep process using readily available and inexpensive alcohols instead of aldehydes as the alkylation reagents. In this context, considerable progress has been directed for the acceptorless dehydrogenative coupling (ADC)

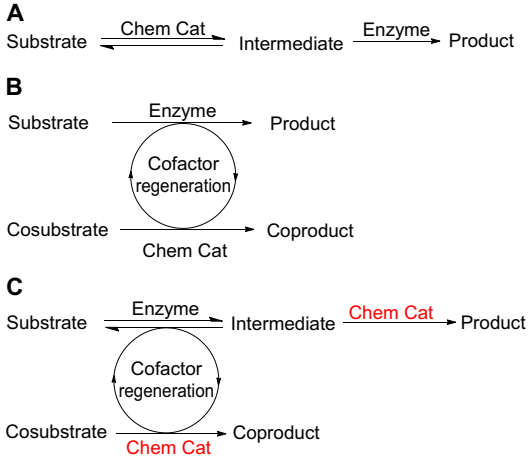

Fig. 1. Overview of CCRs. (**A**) CCR of DKR. (**B**) CCR of cofactor regeneration. (**C**) This work of a novel type of CCR.

[1]College of Biotechnology and Pharmaceutical Engineering, Nanjing Tech University, Nanjing, China. [2]National Engineering Research Center for Biotechnology, Nanjing, China. [3]School of Chemistry and Molecular Engineering, Nanjing Tech University, Nanjing, China.
*Corresponding author. Email: zhucj@njtech.edu.cn

reaction of alcohols with amines due to water and H_2 are only by-products (Fig. 2A) (*23*). Pioneered by Milstein and colleagues (*24*), who reported ruthenium pincer complex as an efficient catalyst for the coupling primary alcohols and amines to amides, various metal pincer complexes have been developed for these conversions (*23*). However, this method still suffers in terms of harsh reaction conditions (high reaction temperature and base and strict anhydrous conditions are often required), complicated synthesis and expensive nature of pincer ligands, often limited with noble-metal catalysts, and potential metal contamination of the products. Hence, the development of an efficient, mild, and environmentally benign synthetic access that can avoid multistep protocols and minimize the waste generation is a demand goal.

Recently, inspired by flavin adenine dinucleotide–containing NADH [reduced form of nicotinamide adenine dinucleotide (NAD^+)] oxidase catalyzing cofactor $NAD(P)^+$ [nicotinamide adenine dinucleotide (phosphate)] regeneration (*25*), we reported the feasibility of $NAD(P)^+$ regeneration system catalyzed by synthetic bridged flavin analog (**SBFA**) in vitro (*26*) and in vivo (*27*). Because of its excellent redox potential and aerobic oxidation characteristic, we speculated whether **SBFA** can be used as a biomimetic organocatalyst for the ADC reaction. Here, we reported a novel cooperative chemoenzymatic type (Fig. 1C) for the synthesis of N-heterocycles under mild reaction conditions catalyzed by a bifunctional biomimetic organocatalyst **SBFA** (Fig. 2B). The role of **SBFA** is not only involved in the cofactor regeneration during the process of alcohol dehydrogenase (ADH)–catalyzed alcohol to aldehyde but also serves as an organocatalyst for the subsequent oxidative condensation reaction between aldehyde and amine. To date, such a chemoenzymatic approach for the synthesis of N-heterocycles has not been reported to the best of our knowledge.

RESULTS

Independent chemo- and biotransformation process catalyzed by SBFA

Chemoprocess for the oxidative condensation of aldehyde and amine catalyzed by **SBFA** was first investigated. Benzaldehyde and phenylenediamine were chosen as the model substrates for the synthesis of 2-phenylbenzimidazole. Four synthetic flavinium derivatives **F1** to **F4** and the natural flavin mononucleotide (FMN) were chosen for comparison. As shown in Table 1, the order of the conversion of the reaction was observed as **F1** > **F2** > **F4** > **F3** > FMN, and this result may be caused by the different redox potentials of the flavin catalysts; the $E^{\circ\prime}$ values of the flavin catalysts decrease in the following order: **F2** ≈ **F1** (−72 mV) > **F4** (−103 mV) > **F3** (−167 mV) > FMN (−219 mV) (*26*), and there seems to be a positive correlation between the catalytic activity and the redox potential of **SBFA**s. The poor catalytic activity of FMN can be attributed to its conformation, which can change from planar to bent during the reduction process (*28*). However, this folding conformational change is not allowed in the case of **SBFA** because of the hindering effect of the N^1, N^{10}-ethylene bridge bond, which is beneficial for accepting hydride from the reaction intermediate (*26*). Control experiment showed that low conversion was observed in the absence of **SBFA** (Table 1, entry 6) and ruled out the possibility of H_2O_2 produced during the reaction process as the terminal oxygen source (Table 1, entry 7).

However, relative to the reasonable reaction conversion, the selectivity of the desired product benzimidazole **1b** was unsatisfactory. By-products including 2-(benzylideneamino)aniline **1d**, 1, 2-disubstituted benzimidazoles **1e**, and its precursor **1f** were always observed during the reaction (Fig. 3B), and this could be attributed to the fast condensation rate between aldehyde and amine. The intermediate **1d** could couple with another molecule of aldehyde to produce **1f**,

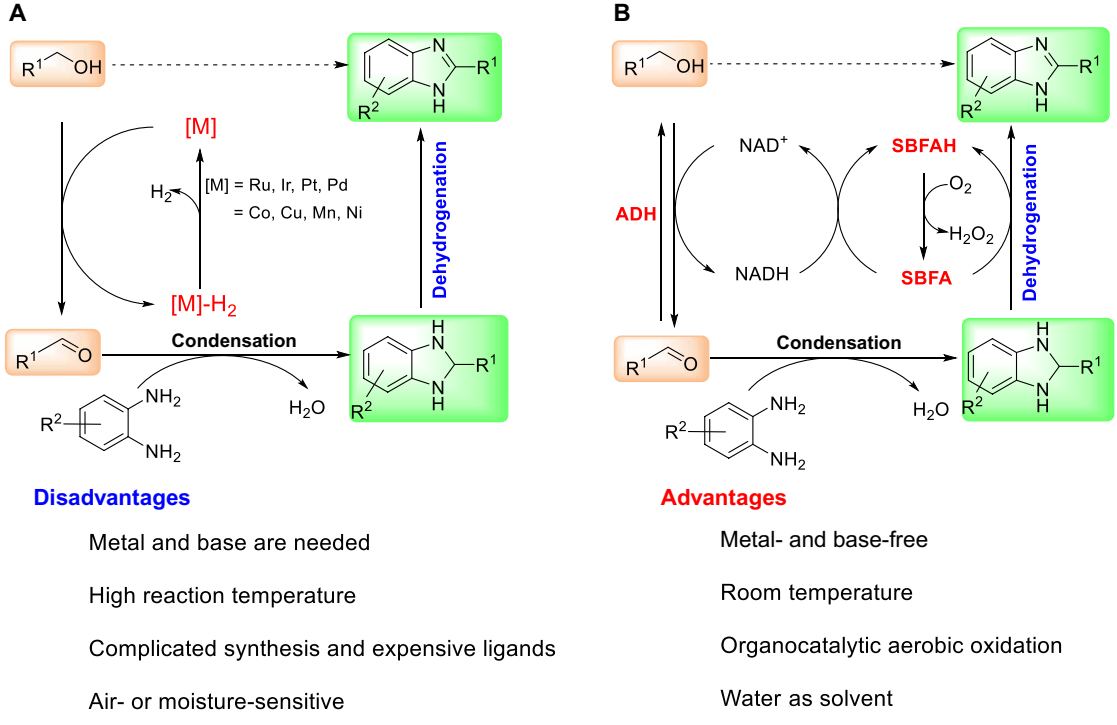

Fig. 2. The different methods for the synthesis of N-heterocycles. (**A**) Previously reported metal-dependent ADC method. (**B**) This work of cooperative chemoenzymatic method.

Table 1. Flavin-mediated synthesis of benzimidazole. Reaction condition: Benzaldehyde (5 mM), 5 mM phenylenediamine, and 0.5 mM **SBFA** were added into 2 ml of water in turn and shaken for 8 hours at 30°C, 200 rpm. PBS, phosphate-buffered saline.

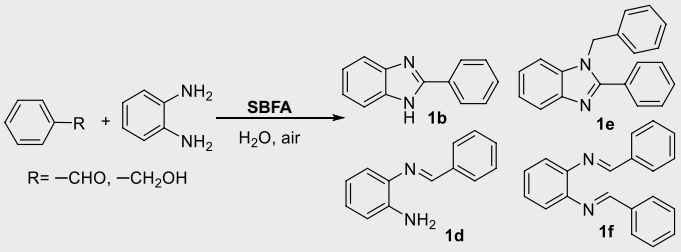

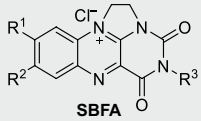

F1: R^1 = H, R^2 = CF_3, R^3 = H
F2: R^1 = H, R^2 = CF_3, R^3 = CH_3
F3: R^1 = H, R^2 = H, R^3 = H
F4: R^1 = Cl, R^2 = H, R^3 = H

Entry	R group	Catalyst/ Reagent	Conversion (%)	Selectivity (%)			
				1b	1d	1e	1f
1	**CHO**	**F1**	78	82	8	7	3
2	**CHO**	**F2**	69	80	9	9	2
3	**CHO**	**F3**	58	88	6	5	1
4	**CHO**	**F4**	63	85	7	6	2
5	**CHO**	**FMN**	51	56	17	12	15
6	**CHO**	–	40	17	27	5	51
7	**CHO**	**H_2O_2**	41	19	26	7	48
8*	**CH_2OH**	**F1**	100	> 99	–	–	–

*Benzyl alcohol (5 mM) was used to replace benzaldehyde. HLADH (0.15 mg/ml) and 1 mM NAD^+ were added into 2 ml of PBS buffer (pH 7.0) and shaken for 24 hours at 30°C, 200 rpm.

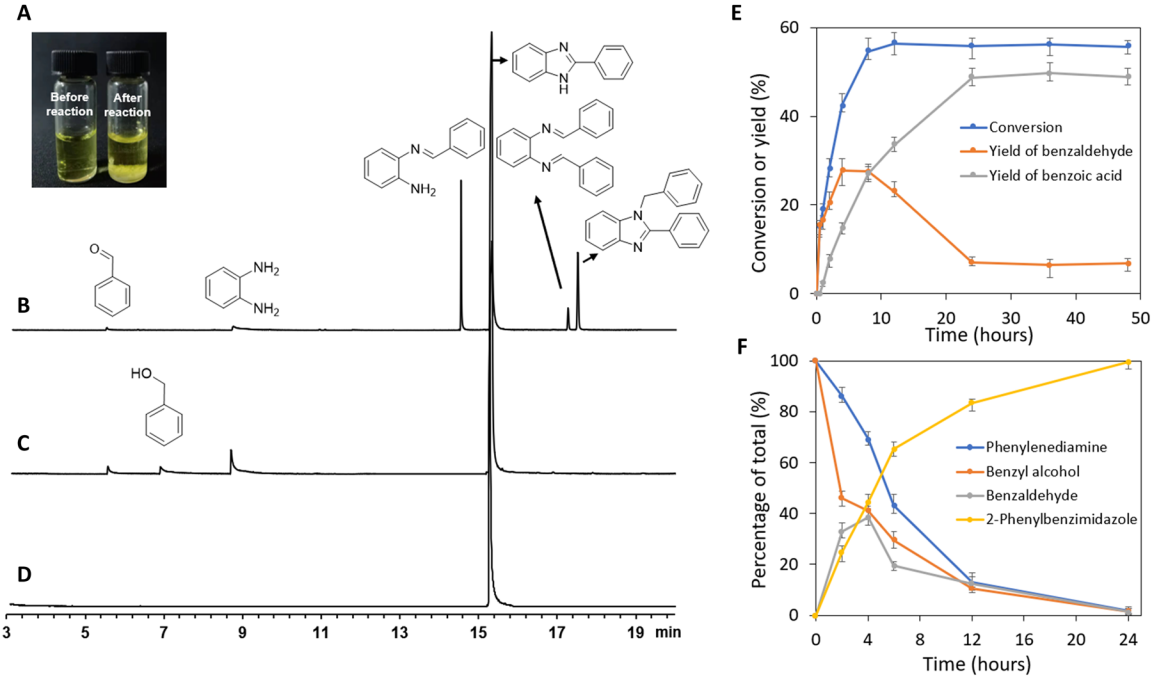

Fig. 3. Individual chemocatalytic, biocatalytic, and cooperative chemoenzymatic synthesis of 2-phenylbenzimidazole. (**A**) The initial state and final state of chemoenzymatic reaction. (**B**) Gas chromatography–mass spectrometry (GC-MS) spectrum of **F1**-catalyzed chemoprocess using benzaldehyde and phenylenediamine as substrates (8 hours) (fig. S2). (**C**) GC-MS spectrum of chemoenzymatic synthesis of 2-phenylbenzimidazole (18 hours). (**D**) GC-MS spectrum of 2-phenylbenzimidazole precipitated from the solution. (**E**) Time course for the biooxidation of benzyl alcohol. (**F**) Time course for the chemoenzymatic synthesis of 2-phenylbenzimidazole.

which subsequently underwent intramolecular cyclization and rearranged to **1e**. Hence, we speculated that gradual generation of aldehyde might be helpful in improving the selectivity of this reaction. To validate the hypothesis, we performed preliminary experiment of horse liver ADH (HLADH)–catalyzed oxidation of benzyl alcohol using **F1** for the in situ regeneration of NAD^+. As shown in Fig. 3E, the conversion of benzyl alcohol and the yield of benzaldehyde increased in the initial stage of the reaction, where maxima values of 56% conversion of benzyl alcohol and 28% yield of benzaldehyde were achieved at 12 and 4 hours, respectively. With further prolongation of the reaction time, the yield of aldehyde decreased, accompanied by the increase of overoxidized product benzoic acid.

Chemoenzymatic synthesis of 2-phenylbenzimidazole in cooperative state

The poor selectivity of chemical synthesis of benzimidazole and the unsatisfactory yield of enzymatic synthesis of benzaldehyde encouraged us to investigate the cooperative chemoenzymatic method to solve this dilemma. Hence, chemoenzymatic synthesis of 2-phenylbenzimidazole using benzyl alcohol and phenylenediamine was then conducted to validate this feasibility, HLADH was used as a biocatalyst to achieve the biotransformation of alcohol into aldehyde, and **F1** served as a bifunctional chemocatalyst for the NAD^+ regeneration and the subsequent oxidative cyclization. We were very pleased to find that under this chemoenzymatic system, the desired product 2-phenylbenzimidazole was obtained in >99% yield (Table 1, entry 8), which was much higher than that of single chemocatalytic process using benzaldehyde as a substrate (>99% versus 64%), thus demonstrating the benefits of a cooperative system over two sequential reactions. This improvement was attributed to the increased reaction selectivity, and none of the by-products such as benzoic acid, **1d**, **1e**, and **1f** were detected during the reaction (Fig. 3C). A typical time course for this chemoenzymatic reaction is shown in Fig. 3F, starting with benzyl alcohol being rapidly consumed within the first 2 hours, yielding the corresponding benzaldehyde, which reacted with phenylenediamine to yield the desired product **1b**. The fast condensation of aldehyde and amine not only avoided the side reaction of the resulting aldehyde being peroxidized to acid but also pulled the direction of the reversible enzymatic reaction toward the generation of aldehyde, thus improving the overall conversion of enzymatic oxidation of alcohol (100% versus 56%). Furthermore, because the aldehyde was gradually produced through bioprocess and constantly being consumed, the concentration of aldehyde always remained at a low level, and the side reaction of double substitution was also avoided. It is worth mentioning that the present chemical catalysis and enzymatic catalysis processes are well compatible with an aqueous reaction system because of the water-soluble characteristics of the organocatalyst **F1**, which also offers convenience for the separation of the product. Isolation of products from the reaction media is often a tedious procedure in chemoenzymatic system; for the present system, the desired product 2-phenylbenzimidazole was precipitated from the solution with close to 100% purity due to its poor water solubility (Fig. 3, A and D). It can be purified by simple filtration and washing, thus getting rid of the conventional separation processes such as extraction or column chromatography.

Substrate scope for benzimidazoles

To evaluate the versatility of this chemoenzymatic method, we applied the procedure for the synthesis of a variety of substituted benzimidazoles using alcohols as substrates (method A in Fig. 4A); the chemoprocess using aldehydes as substrates was also conducted for the comparison (method B in Fig. 4A). As can be seen in Fig. 4A, most alcohols underwent smooth transformation under a chemoenzymatic system to afford the corresponding benzimidazoles in excellent yields, and the yields of chemoenzymatic method are generally higher than those of chemocatalytic method. The electronic properties of the substituents of benzylic alcohols had a remarkable influence on the reaction. Electron-donating groups, such as $-OCH_3$ group, enhanced the cyclization step because of the decreased electrophilicity of the carbonyl carbon atom; for example, 2-(4-methoxyphenyl)benzimidazole (**2b**) could be obtained with the yield of >99% in 4 hours. However, for the transformation of electron-withdrawing group that substituted benzyl alcohol, the chemoenzymatic method was not successful, although a moderate yield of 69% of the corresponding chemocatalytic process was achieved (**3b**), which was due to the fact that HLADH could not catalyze the conversion of 4-nitrobenzyl alcohol to 4-nitrobenzaldehyde (fig. S3). Although excellent chemoselectivity was observed for the method A system, no noticeable overoxidation of aldehyde to carboxylic acid was detected during the reaction. As the functional groups, such as oxidation-sensitive allylic alcohol, was transformed efficiently without any observable reaction at the double-bond functionality (**4b**). Heterocyclic alcohol including 2-(hydroxymethyl)pyridine, furfuryl alcohol, and 2-thiophenemethanol also gave moderate to excellent yields (**5b** to **7b**). Notably, together with the good results with benzylic, allylic, and heteroaryl alcohols, the yields obtained from the reaction of naphthenic and aliphatic alcohols are also quite high (**8b** and **9b**). In view of the fact that the reaction of aliphatic alcohol is much more difficult than the reaction of benzylic alcohol (*29*), the results obtained using the present procedure were very satisfactory. The different catalytic activities between the chemoenzymatic and chemocatalytic methods observed in Fig. 4A is attributed to two aspects: The first is to reduce the generation of by-products such as disubstituted products during the chemocatalytic process, thus improving the selectivity of the reaction; the other is to drive the direction of the reversible enzymatic reaction toward the aldehyde production pathway and to reduce the side reaction of aldehyde peroxidation to acid (*30*, *31*), thus improving the yield of the aldehyde and, in turn, promote the whole cascade reaction. It should be noted that in the independent process of enzyme catalysis, the yields of aldehydes were generally not more than 60% (fig. S3). This cooperative effect of multiple catalysts led to enhanced reactivity and outcomes that could not be achieved by the sequential application of individual catalysts perfectly embodying the advantages of the CCR. To further demonstrate the practical relevance of this cooperative chemoenzymatic system, we applied it for the synthesis of drug pimobendan, which is a calcium sensitizer drug for the treatment of chronic heart failure, ischemic heart disease, and arterial tlirombotic diseases (*32*). Under this nonoptimized condition, 53% overall yield of pimobendan could be achieved in 24 hours, and this moderate yield was ascribed to the poor solubility of diamine in water.

Chemoenzymatic synthesis of other N-heterocycles

With the aim of developing and defining the scope and limitation of this cooperative chemoenzymatic method, the HLADH-**F1** catalytic system was then extended for the synthesis of other typical N-heterocycles, ranging from pyrazine to quinazoline, indole, and quinoline; these important skeletons are frequently found as the core fragments of

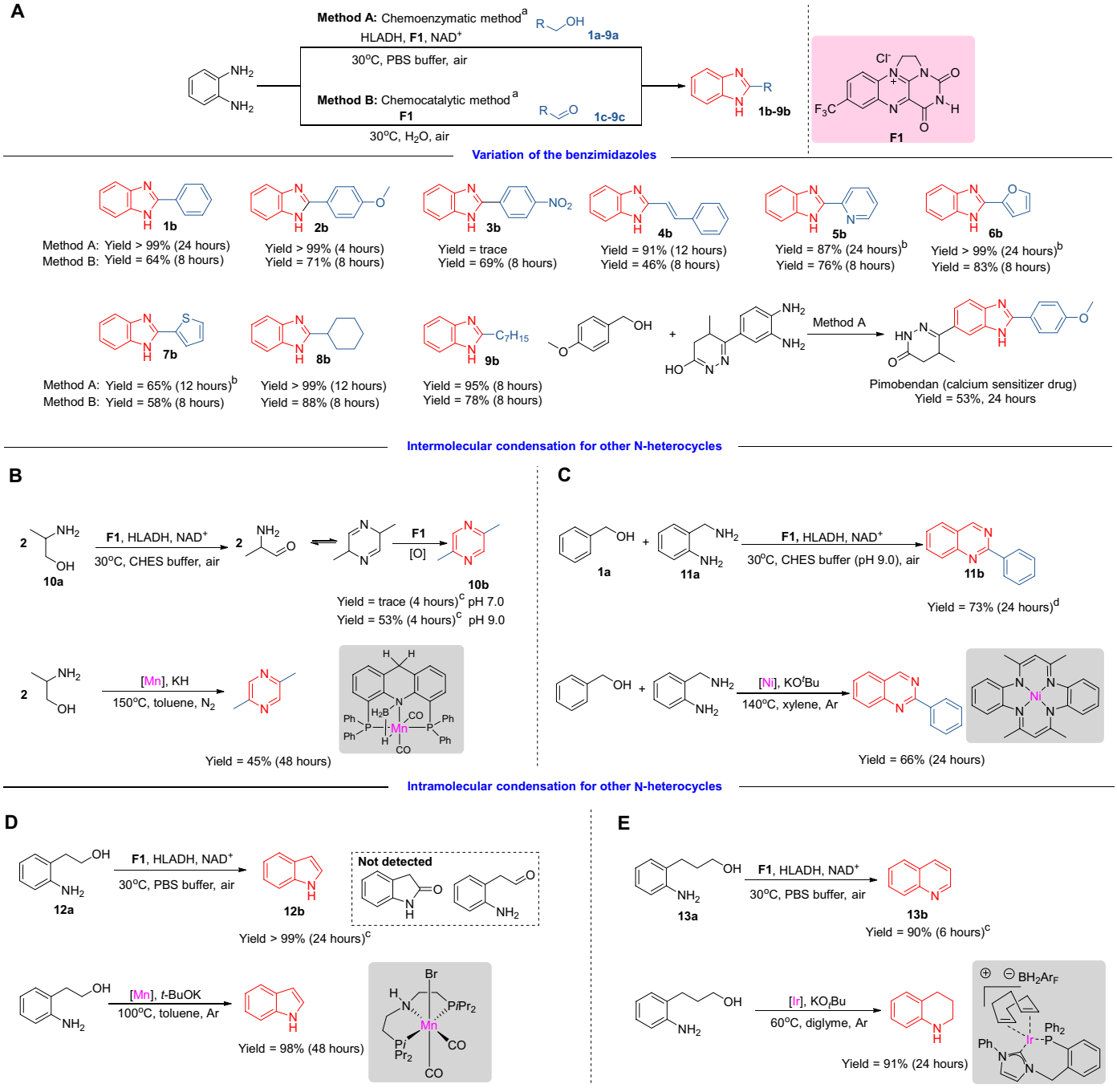

Fig. 4. Reaction scope of CCR for the synthesis of various N-heterocycles. (**A**) CCR for the synthesis of benzimidazoles. PBS, phosphate-buffered saline. (**B**) CCR versus ADC method for the synthesis of pyrazine. CHES, N-Cyclohexyl-2-aminoethanesulfonic acid. (**C**) CCR versus ADC method for the synthesis of quinazoline. (**D**) CCR versus ADC method for the synthesis of indole. (**E**) CCR versus ADC method for the synthesis of quinoline. [a]Method A: HLADH (0.15 mg/ml), 5 mM alcohols, 5 mM diamine, 0.5 mM **F1**, and 1 mM NAD^+ were added in 2 ml of 100 mM PBS buffer (pH 7.0) in turn and shaken at 30°C, 200 rpm; Method B: 5 mM aldehydes, 5 mM diamine, and 0.5 mM **F1** were added into 2 ml of water in turn and shaken at 30°C, 200 rpm. [b]**F1** was 1 mM. [c]Corresponding substates (10 mM) were used, while other conditions were referred to method A unless otherwise noted. [d]Using method A.

pharmaceuticals, natural products, bioactive compounds, and functional materials (*33*, *34*).

The intermolecular condensation reactions for the synthesis of pyrazine (Fig. 4B) and quinazoline (Fig. 4C) were first explored. Using 2-aminopropanol as a substrate, only a trace amount of the desired product 2,5-dimethylpyrazine (DMP) was observed under the original reaction condition (pH 7.0), and increasing the concentration of HLADH or **F1** or reaction temperature did not show any improvement. However, by increasing pH value of the reaction mixture up to 9.0, DMP could be obtained with the yield of 53% (Fig. 4B and fig. S4). To find out the specific reason for this pH-dependent phenomenon, the control experiment about the effect

of pH (from 6.0 to 9.0) on the HLADH-catalyzed oxidation of 2-aminopropanol was carried out. As shown in fig. S5, the reaction cannot proceed under acidic conditions, and the conversion of 2-aminopropanol increases along with the pH value. Thus, we can confirm that the rather low affinity of HLADH toward 2-aminopropanol at lower pH values is the main reason affecting the whole cascade reaction, which probably due to the protonated amines affects the recognition by HLADH, and this result is in line with HLADH-catalyzed oxidative lactamization of amino alcohols recently reported by Kara's group (*35*). To date, ADC reaction catalyzed by diversity of well-designed metal complex represents an effective and straightforward method for the synthesis of pyrazines. Compared with the same reaction catalyzed by metal manganese pincer complexes (Fig. 4B) (*36*), being metal and base free, requiring only water as solvent, not needing inert atmosphere, having short reaction time, and mild reaction conditions were observed for the present chemoenzymatic method. Recently, Kroutil's group (*37*) also reported a chemoenzymatic synthesis of DMP by transaminase-catalyzed deamination of 1,2-diaminopropane using pyruvate as the amine acceptor, with 1,4-dichlorobenzoquione used as a chemocatalyst for the following oxidative aromatization. However, a low conversion of 27% was obtained in 72 hours.

The construction of quinazoline was further tested to verify the applicability of the present chemoenzymatic method. As shown Fig. 4C, the desired product 2-phenylquinazoline was obtained in 73% of yield in 24 hours by condensation of benzyl alcohol and 2-aminobenzylamine, and obvious advantages were still observed compared with the nickel complex–catalyzed ADC reaction of the same substrates (Fig. 4C) (*38*). To the best of our knowledge, this is the first example of chemoenzymatic synthesis of quinazoline. However, further attempts for synthesis of quinoxaline and pyrrole using glycol or 2, 5-hexanediol as a substrate were not successful because HLADH failed to oxidize diol (fig. S6 and S7).

Apart from intermolecular cyclization, intramolecular condensation reactions were further performed (Fig. 4, D and E). As shown in Fig. 4D, using 2-(2-aminophenyl)ethanol as a substrate, 99% yield of 1*H*-indole could be obtained through tautomerization of 3*H*-indole driven by spontaneous aromatization under the present chemoenzymatic system. It is worth mentioning that whereas excellent chemoselectivity was observed for the present chemoenzymatic system, neither overoxidated by-product indolin-2-one nor hydrolytic by-product 2-(2-aminophenyl)acetaldehyde was detected during the reaction (fig. S8). Compared with the same reaction catalyzed by metal manganese pincer complexes (Fig. 4D) (*39*), obvious advantages were also observed for the present chemoenzymatic method. Castagnolo's group (*40*) recently reported a chemoenzymatic method for the synthesis of indole derivatives. Indolines were first prepared via photocatalytic cyclization of arylaniline precursors and, in turn, catalyzed by monoamine oxidase (MAO-N) to afford indoles. Although this approach exhibited broad substrate scope with good to excellent yields, it needed more than 7 days to complete the whole chemoenzymatic process because of the low oxidation efficiency of MAO-N.

To further verify this method in the construction of six-membered ring, we then applied the present chemoenzymatic system to the synthesis of quinoline. Starting from 3-(2-aminophenyl)propanol, quinoline could be obtained in 90% of yield in 6 hours (Fig. 4E). Common by-products such as 1,2,3,4-tetrahydroquinoline, 3,4-dihydroquinoline, and quinolone, those often observed in metal-catalyzed ADC reactions, were not detected under the present system (fig. S9) (*41*). It is worth mentioning that tetrahydroquinoline is the main product in most metal-catalyzed ADC reactions (Fig. 4E) (*42*) because the intermediate 3,4-dihydroquinoline could not be dehydrogenated by those catalytic systems. To the best of our knowledge, this is also the first example of chemoenzymatic synthesis of quinoline. However, further attempts to synthesize isoquinoline were unsuccessful because the HLADH could not catalyze [2-(2-aminoethyl)phenyl]-methanol to the corresponding aldehyde (fig. S10).

Mechanistic study of chemoprocess catalyzed by SBFA

As shown in Fig. 5A, the reaction pathway can be divided into two parts: the biocatalysis and chemocatalysis parts. In the biocatalysis part, alcohol was biotransformed to aldehyde by HLADH at the cost of continuously consumed NAD^+, which was in situ–regenerated by **F1**. The formed **F1H** was oxidized by oxygen, releasing hydrogen peroxide to complete the cycle. In the chemocatalysis part, the generated aldehyde was spontaneously condensed with diamine to form imine intermediate **i**, which underwent cyclization to produce benzimidazoline **j**. Last, under the redox catalytic system, oxidation of **j** afforded the desired benzimidazole with concurrent regeneration of **F1** to continue the whole catalytic cycle.

In the classic ADC reaction, metal hydride is considered as an important intermediate (*43*); the isolation and characterization of intermediate **F1H** as an air-sensitive compound was achieved during biocatalysis process (fig. S17), and a hydride transfer mechanism between **F1** and NADH was proposed in our previous study (*26*). However, the detailed redox pathway of **F1**-catalyzed chemoprocess is still unclear but highly desired. According to the mechanistic studies of amine oxidation catalyzed by MAO-N (*44*), two challenging issues have mainly inhibited the exploration of the chemocatalytic mechanism: (i) The initial step in the reductive half-reaction: single-electron transfer (SET) or hydride transfer (can be further subdivided into direct hydride transfer from the αC of intermediate **j** to the N5 of **F1** or two-step hydride transfer with the formation of N5 adduct) or polar nucleophilic mechanism through C4a addition followed by intramolecular deprotonation. (ii) The regioselectivity of oxygen addition in the oxidative half-reaction: C4a or C10a position of flavin (Fig. 5A). Thereby, further experiments have been conducted to offer deeper understanding of the abovementioned steps. Initially, the results of radical-trapping experiments by using 2,2,6,6-Tetramethylpiperidinooxy (TEMPO) or Butylated Hydroxytoluene (BHT) as a radical scavenger first ruled out the possibility of the SET mechanism (fig. S11). Next, the density functional theory (DFT) calculations were performed to evaluate the remaining three pathways (fig. S12). According to the results of relaxed potential energy scan, the N5 adduct and C4a adduct intermediates both were not available because of the much higher energy barrier (fig. S13), which was probably ascribed to the large steric hindrance. Hence, the direct hydride transfer from the αC of intermediate **j** to the N5 of **F1** was proposed for the reductive half-reaction, traversing the transition state TS1 with a barrier of 13.2 kcal/mol to give rise to IM2 (intermediate 2), and the optimized energy profile was depicted in Fig. 5B.

The detailed reaction pathway for the subsequent regeneration of **F1** is also subject to controversy, as two possible routes are under consideration (fig. S14), one of which is that the reduced flavin **F1H** was reoxidized via a sequence of disproportionations and two successive SETs to O_2 through a C4a-flavin hydroperoxide adduct, as usually known for the natural flavin regenerated by O_2 (*45*).

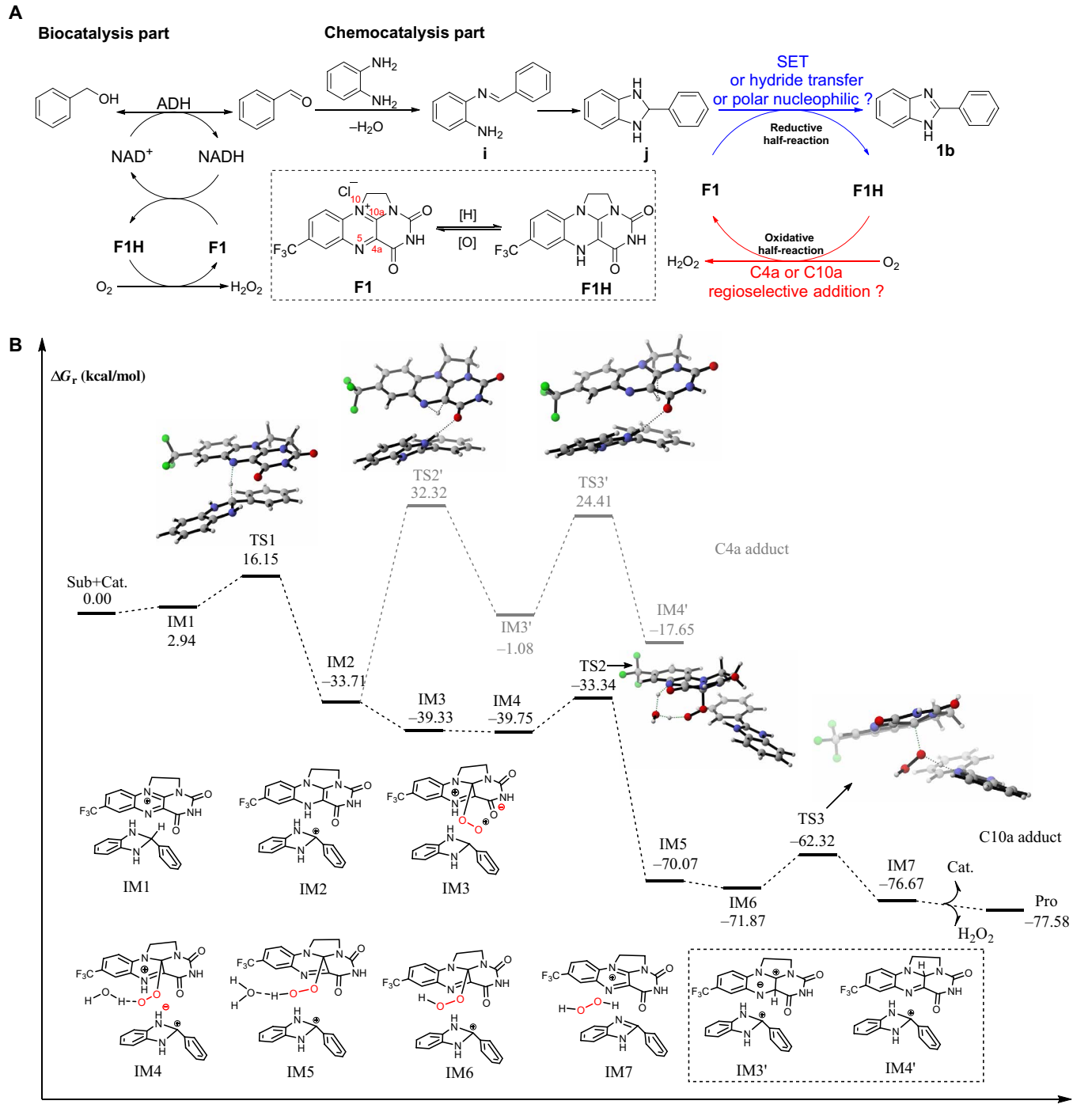

Fig. 5. The pathway and mechanism analysis of F1-mediated chemoenzymatic synthesis of benzimidazole. (**A**) The reaction pathway of chemoenzymatic synthesis of 2-phenylbenzimidazole. (**B**) DFT analysis of **F1**-catalyzed oxidation of chemoprocess.

However, according to our recent study (*26*), another route through a C10a-flavin hydroperoxide adduct for **F1** was also possible, which is different from the regeneration mechanism of natural flavin. To gain deep insight into the regioselective addition step, we further explored DFT calculations (Fig. 5B). As illustrated in Fig. 5B, the comparison of activation barriers shows that energy barrier through C4a adduct was about 10 times higher than that of C10a adduct (66.03 versus 6.41 kcal/mol). Notably, the proposed H_2O_2 by-product in a C10a-oxidative approach has been confirmed in the redox reaction (fig. S15). Collectively, all the data indicated that the regioselective C10a addition was involved in the oxidative half-reaction.

On the basis of the above results, a possible catalytic cycle for the chemocatalysis part was depicted in Fig. 6. Initially, the direct hydride transfer from the αC of intermediate **j** to the N5 of **F1** was conducted, which produced the key catalyst **F1H** along with the cationic intermediate **A**. Subsequently, regioselective C10a addition of O_2 to **F1H**

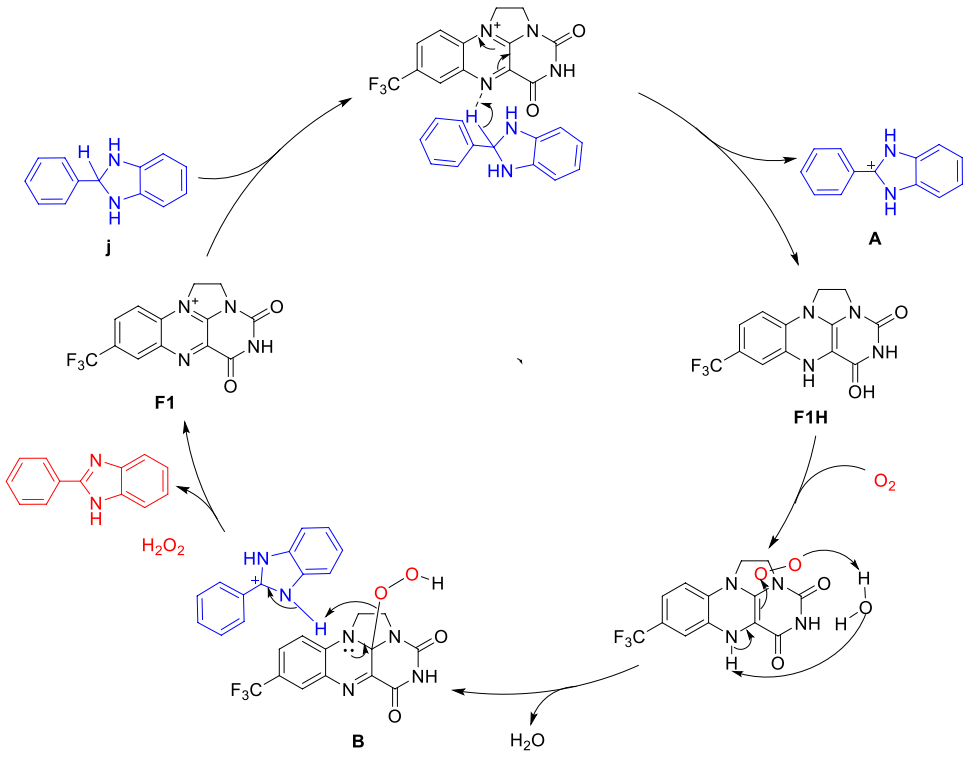

Fig. 6. The possible mechanism of F1-catalyzed chemical synthesis of 2-phenylbenzimidazole.

occurred to generate the hydroperoxide adduct **B** with the assistance of H_2O. Last, the proton transfer from the cationic intermediate **A** to oxidative **B** afforded the desired 2-phenylbenzimidazole product with concurrent regeneration of the active **F1** catalyst.

DISCUSSION

We have developed a novel, convenient, and efficient two-step, one-pot cooperative chemoenzymatic process for the synthesis of N-heterocycles directly from alcohols and amines. Organocatalyst **F1** acting as a bifunctional catalyst, which played dual roles in both bio- and chemoprocesses, was first reported. The cooperative effect of chemocatalyst **F1** and biocatalyst HLADH led to enhanced reactivity and outcomes that could not be achieved by the sequential application of individual catalysts that perfectly embodied the advantages of cooperative chemoenzymatic process. A wide range of valuable scaffolds including benzimidazole, pyrazine, quinazoline, indole, and quinoline can be obtained in excellent yields under mild reaction conditions. Mechanistic studies revealed that direct hydride transfer and C10a addition occurred during the reductive and oxidative half-reaction of **F1**. The present work not only offers a promising strategy for the construction of N-heterocycles but also expands the scope of chemoenzymatic process, which will inspire the integration of organocatalysts and biocatalysts for the manufacture of bulk and fine chemicals.

MATERIALS AND METHODS

General procedure for chemical synthesis of benzimidazole derivatives

In a test tube (5 ml), 5 mM aldehydes, 5 mM *o*-phenylenediamine, and 0.5 mM natural flavin or **SBFA** were added into 2 ml of water in turn and shaken at 30°C, 200 rpm. The samples were taken at interval times, extracted with EtOAc, and then dried over anhydrous $MgSO_4$ for the gas chromatography–mass spectrometry (GC-MS) or high-performance liquid chromatography (HPLC) determination.

General procedure for the oxidation of alcohols with the F1-HLADH system

In a test tube (5 ml), the purified HLADH (0.15 mg/ml) was suspended in 2 ml of 50 mM phosphate-buffered saline (pH 7.0). Then, 5 mM alcohols, 0.5 mM **F1**, and 1 mM NAD^+ were added in turn and shaken at 30°C, 200 rpm. The samples were taken at interval times, extracted with EtOAc, and then dried over anhydrous $MgSO_4$ for GC or HPLC determination.

General procedure for one-pot cooperative chemoenzymatic synthesis of N-heterocycles

For the synthesis of benzimidazole derivatives and quinazoline: In a test tube, the purified HLADH (0.15 mg/ml) was suspended in 50 mM buffer. Then, 5 mM alcohols, 5 mM diamine, 0.5 mM **F1**, and 1 mM NAD^+ were added in turn and shaken at 30°C, 200 rpm. For the synthesis of pyrazine, indole, and quinoline: Aminoalcohols substrates (10 mM) were used, and the other conditions and reagents of reaction were the same as above. All the samples were taken at interval times, extracted with EtOAc, and then dried over anhydrous $MgSO_4$ for GC-MS, GC, or HPLC determination.

DFT calculation

The mechanism was investigated via DFT using the M06-2X functional (*46*) with the 6-31 + G(d, p) basis sets as implemented in Gaussian 16 package (*47*), which was used in the geometric optimizations of intermediates and transition states. To check the intermediate

and transition state structures, vibrational frequency calculations at the same level of theory were performed, and for the local minima, there are no imaginary frequencies, while, for the transition states, one imaginary frequency can be found. Intrinsic reaction coordinates (*48*, *49*) were performed to confirm the transition states connecting with the corresponding reactant and product intermediates. During the quantum mechanical calculations, the integral equation formalism for the polarizable continuum model (*50*–*52*), solvent model for water was chosen to mimic the role of the active site in stabilizing charges. Thermochemistry corrections to achieve the free energies and enthalpies were computed at 298 K and 1 M, with Truhlar corrections applied to all frequencies below 100 cm^{-1}. In all mechanisms, the energies are the Gibbs free energies. To obtain more accurate energetics, single-point energy calculations were performed on the optimized structures at the M06-2X/6–311++G(2d,2p) level of theory (tables S1 and S2).

SUPPLEMENTARY MATERIALS

Supplementary material for this article is available at https://science.org/doi/10.1126/sciadv.add1912

REFERENCES AND NOTES

1. J. H. Schrittwieser, S. Velikogne, M. Hall, W. Kroutil, Artificial biocatalytic linear cascades for preparation of organic molecules. *Chem. Rev.* **118**, 270–348 (2017).
2. J. M. Sperl, V. Sieber, Multienzyme cascade reactions-status and recent advances. *ACS Catal.* **8**, 2385–2396 (2018).
3. R. Sigrist, B. Z. da Costa, A. J. Marsaioli, L. G. de Oliveira, Nature-inspired enzymatic cascades to build valuable compounds. *Biotechnol. Adv.* **33**, 394–411 (2015).
4. F. Rudroff, M. D. Mihovilovic, H. Gröger, R. Snajdrova, H. Iding, U. T. Bornscheuer, Opportunities and challenges for combining chemo- and biocatalysis. *Nat. Catal.* **1**, 12–22 (2018).
5. X. Huang, M. Cao, H. Zhao, Integrating biocatalysis with chemocatalysis for selective transformations. *Curr. Opin. Chem. Biol.* **55**, 161–170 (2020).
6. V. Köhler, N. J. Turner, Artificial concurrent catalytic processes involving enzymes. *Chem. Commun.* **51**, 450–464 (2015).
7. J. Muschiol, C. Peters, N. Oberleitner, M. D. Mihovilovic, U. T. Bornscheuer, F. Rudroff, Cascade catalysis - Strategies and challenges En route to preparative synthetic biology. *Chem. Commun.* **51**, 5798–5811 (2015).
8. Z. C. Litman, Y. Wang, H. Zhao, J. F. Hartwig, Cooperative asymmetric reactions combining photocatalysis and enzymatic catalysis. *Nature* **560**, 355–359 (2018).
9. O. Verho, J.-E. Bäckvall, Chemoenzymatic dynamic kinetic resolution: A powerful tool for the preparation of enantiomerically pure alcohols and amines. *J. Am. Chem. Soc.* **137**, 3996–4009 (2015).
10. X. Wang, H. H. P. Yiu, Heterogeneous catalysis mediated cofactor NADH regeneration for enzymatic reduction. *ACS Catal.* **6**, 1880–1886 (2016).
11. J. S. DeHovitz, Y. Y. Loh, J. A. Kautzky, K. Nagao, A. J. Meichan, M. Yamauchi, D. W. C. Macmillan, T. K. Hyster, Static to inducibly dynamic stereocontrol: The convergent use of racemic β-substituted ketones. *Science* **369**, 1113–1118 (2020).
12. Y. Wang, X. Huang, J. Hui, L. T. Vo, H. Zhao, Stereoconvergent reduction of activated alkenes by a nicotinamide free synergistic photobiocatalytic system. *ACS Catal.* **10**, 9431–9437 (2020).
13. C. A. Denard, J. F. Hartwig, H. Zhao, Multistep one-pot reactions combining biocatalysts and chemical catalysts for asymmetric synthesis. *ACS Catal.* **3**, 2856–2864 (2013).
14. M. Poizat, I. W. C. E. Arends, F. Hollmann, On the nature of mutual inactivation between $[Cp^*Rh(bpy)(H_2O)]^{2+}$ and enzymes – Analysis and potential remedies. *J. Mol. Catal. B Enzym.* **63**, 149–156 (2010).
15. F. Hildebrand, S. Lütz, Stable electroenzymatic processes by catalyst separation. *Chem. A Eur. J.* **15**, 4998–5001 (2009).
16. F. Pozharskii, A. T. Soldatenkov, A. R. Katritzky, *Heterocycles in Life and Society: An Introduction to Heterocyclic Chemistry, Biochemistry and Applications* (Wiley, 2011).
17. H. Gao, Q. Zhang, J. M. Shreeve, Fused heterocycle-based energetic materials (2012–2019). *J. Mater. Chem. A* **8**, 4193–4216 (2020).
18. E. Vitaku, D. T. Smith, J. T. Njardarson, Analysis of the structural diversity, substitution patterns, and frequency of nitrogen heterocycles among U.S. FDA approved pharmaceuticals. *J. Med. Chem.* **57**, 10257–10274 (2014).
19. P. R. Nitha, S. Soman, J. John, Indole fused heterocycles as sensitizers in dye-sensitized solar cells: An overview. *Mater. Adv.* **2**, 6136–6168 (2021).
20. X. Wen, J. E. Bakali, R. Deprez-Poulain, B. Deprez, Efficient propylphosphonic anhydride (®T3P) mediated synthesis of benzothiazoles, benzoxazoles and benzimidazoles. *Tetrahedron Lett.* **53**, 2440–2443 (2012).
21. R. Thakur, Y. Jaiswal, A. Kumar, Imidates: An emerging synthon for N-heterocycles. *Org. Biomol. Chem.* **17**, 9829–9843 (2019).
22. B. Han, X. L. Yang, C. Wang, Y. W. Bai, T. C. Pan, X. Chen, W. Yu, CuCl/DABCO/4-HO-TEMPO-catalyzed aerobic oxidative synthesis of 2-substituted Quinazolines and 4H-3,1-benzoxazines. *J. Org. Chem.* **77**, 1136–1142 (2012).
23. C. Gunanathan, D. Milstein, Applications of acceptorless dehydrogenation and related transformations in chemical synthesis. *Science* **341**, 1229712 (2013).
24. C. Gunanathan, Y. Ben-David, D. Milstein, Direct synthesis of amides from alcohols and amines with liberation of H_2. *Science* **317**, 790–792 (2007).
25. C. Nowak, B. C. Beer, A. Pick, T. Roth, P. Lommes, V. Sieber, A water-forming NADH oxidase from lactobacillus pentosus suitable for the regeneration of synthetic biomimetic cofactors. *Front. Microbiol.* **6**, 957 (2015).
26. C. Zhu, Q. Li, L. Pu, Z. Tan, K. Guo, H. Ying, P. Ouyang, Nonenzymatic and metal-free organocatalysis for in situ regeneration of oxidized cofactors by activation and reduction of molecular oxygen. *ACS Catal.* **6**, 4989–4994 (2016).
27. Z. Tan, C. Zhu, J. Fu, X. Zhang, M. Li, W. Zhuang, H. Ying, Regulating cofactor balance in vivo with a synthetic flavin analogue. *Angew. Chem. Int. Ed. Engl.* **57**, 16464–16468 (2018).
28. P. Hemmerich, C. Veeger, H. C. S. Wood, Progress in the chemistry and molecular biology of flavins and flavocoenzymes. *Angew. Chem. Int. Ed. Engl.* **4**, 671–687 (1965).
29. K. Bahrami, M. M. Khodaei, A. Nejati, Synthesis of 1,2-disubstituted Benzimidazoles, 2-substituted Benzimidazoles and 2-substituted Benzothiazoles in SDS Micelles. *Green Chem.* **12**, 1237–1241 (2010).
30. P. Könst, H. Merkens, S. Kara, S. Kochius, A. Vogel, R. Zuhse, D. Holtmann, I. W. C. E. Arends, F. Hollmann, Enantioselective oxidation of aldehydes catalyzed by alcohol dehydrogenase. *Angew. Chem. Int. Ed. Engl.* **51**, 9914–9917 (2012).
31. H. Jia, M. Zong, H. Yu, N. Li, Dehydrogenase-catalyzed oxidation of furanics: Exploitation of hemoglobin catalytic promiscuity. *ChemSusChem* **10**, 3524–3528 (2017).
32. J. C. A. Van Meel, A. B. M. Mauz, W. Wienen, W. Diederen, Pimobendan increases survival of cardiomyopathic hamsters. *J. Cardiovasc. Pharmacol.* **13**, 508–509 (1989).
33. M. Baumann, I. R. Baxendale, S. V. Ley, N. Nikbin, An overview of the key routes to the best selling 5-membered ring heterocyclic pharmaceuticals. *Beilstein J. Org. Chem.* **7**, 442–495 (2011).
34. M. M. Heravi, V. Zadsirjan, Prescribed drugs containing nitrogen heterocycles: An overview. *RSC Adv.* **10**, 44247–44311 (2020).
35. L. Huang, G. V. Sayoga, F. Hollmann, S. Kara, Horse liver alcohol dehydrogenase-catalyzed oxidative lactamization of amino alcohols. *ACS Catal.* **8**, 8680–8684 (2018).
36. P. Daw, A. Kumar, N. A. Espinosa-Jalapa, Y. Diskin-Posner, Y. Ben-David, D. Milstein, Synthesis of pyrazines and quinoxalines via acceptorless dehydrogenative coupling routes catalyzed by manganese pincer complexes. *ACS Catal.* **8**, 7734–7741 (2018).
37. S. E. Payer, J. H. Schrittwieser, W. Kroutil, Vicinal diamines as smart cosubstrates in the transaminase-catalyzed asymmetric amination of ketones. *Eur. J. Org. Chem.* **2017**, 2553–2559 (2017).
38. S. Parua, R. Sikari, S. Sinha, G. Chakraborty, R. Mondal, N. D. Paul, Accessing polysubstituted quinazolines via nickel catalyzed acceptorless dehydrogenative coupling. *J. Org. Chem.* **83**, 11154–11166 (2018).
39. S. Elangovan, J. Neumann, J. B. Sortais, K. Junge, C. Darcel, M. Beller, Efficient and selective *N*-alkylation of amines with alcohols catalysed by manganese pincer complexes. *Nat. Commun.* **7**, 12641–12648 (2016).
40. F. Zhao, D. Masci, S. Ferla, C. Varricchio, A. Brancale, S. Colonna, G. W. Black, N. J. Turner, D. Castagnolo, Monoamine oxidase (MAO-N) biocatalyzed synthesis of indoles from indolines prepared via photocatalytic cyclization/arylative dearomatization. *ACS Catal.* **10**, 6414–6421 (2020).
41. J. Li, P. G. Andersson, Room temperature and solvent-free iridium-catalyzed selective alkylation of anilines with alcohols. *Chem. Commun.* **49**, 6131–6133 (2013).
42. K. Fujita, K. Yamamoto, R. Yamaguchi, Oxidative cyclization of amino alcohols catalyzed by a Cp^*Ir complex. Synthesis of Indoles, 1,2,3,4-tetrahydroquinolines, and 2,3,4,5-tetrahydro-1-benzazepine. *Org. Lett.* **4**, 2691–2694 (2002).
43. K. Chakrabarti, M. Maji, S. Kundu, Cooperative iridium complex-catalyzed synthesis of quinoxalines, benzimidazoles and quinazolines in water. *Green Chem.* **21**, 1999–2004 (2019).
44. V. F. Batista, J. L. Galman, D. C. G. A. Pinto, A. M. S. Silva, N. J. Turner, Monoamine oxidase: Tunable activity for amine resolution and functionalization. *ACS Catal.* **8**, 11889–11907 (2018).
45. P. Pimviriyakul, P. Chaiyen, Overview of flavin-dependent enzymes, in *The Enzymes*, P. Chaiyen, F. Tamanoi, Eds. (Elsevier, 2020), chap. 1, vol. 47, pp. 1–36.
46. M. J. Frisch, G. W. Trucks, H. B. Schlegel, G. W. Trucks, H. B. Schlegel, G. E. Scuseria, M. A. Robb, J. R. Cheeseman, G. Scalmani, V. Barone, G. A. Petersson, H. Nakatsuji, X. Li,

M. Caricato, A. V. Marenich, J. Bloino, B. G. Janesko, R. Gomperts, B. Mennucci, H. P. Hratchian, J. V. Ortiz, A. F. Izmaylov, J. L. Sonnenberg, D. Williams-Young, F. Ding, F. Lipparini, F. Egidi, J. Goings, B. Peng, A. Petrone, T. Henderson, D. Ranasinghe, V. G. Zakrzewski, J. Gao, N. Rega, G. Zheng, W. Liang, M. Hada, M. Ehara, K. Toyota, R. Fukuda, J. Hasegawa, M. Ishida, T. Nakajima, Y. Honda, O. Kitao, H. Nakai, T. Vreven, K. Throssell, J. A. Montgomery, Jr., J. E. Peralta, F. Ogliaro, M. J. Bearpark, J. J. Heyd, E. N. Brothers, K. N. Kudin, V. N. Staroverov, T. A. Keith, R. Kobayashi, J. Normand, K. Raghavachari, A. P. Rendell, J. C. Burant, S. S. Iyengar, J. Tomasi, M. Cossi, J. M. Millam, M. Klene, C. Adamo, R. Cammi, J. W. Ochterski, R. L. Martin, K. Morokuma, O. Farkas, J. B. Foresman, D. J. Fox, *Gaussian 16, Revision A.03* (Gaussian Inc., 2016).

47. Y. Zhao, D. G. Truhlar, The M06 suite of density functionals for main group thermochemistry, thermochemical kinetics, noncovalent interactions, excited states, and transition elements: Two new functionals and systematic testing of four M06-class functionals and 12 other functionals. *Theor. Chem. Acc.* **120**, 215–241 (2008).
48. H. P. Hratchian, H. B. Schlegel, Accurate reaction paths using a hessian based predictor–corrector integrator. *J. Chem. Phys.* **120**, 9918–9924 (2004).
49. H. P. Hratchian, H. B. Schlegel, Using Hessian updating to increase the efficiency of a Hessian based predictor-corrector reaction path following method. *J. Chem. Theo. Comput.* **1**, 61–69 (2005).
50. S. Miertuš, E. Scrocco, J. Tomasi, Electrostatic interaction of a solute with a continuum. A direct utilizaion of AB initio molecular potentials for the prevision of solvent effects. *Chem. Phys.* **55**, 117–129 (1981).
51. S. Miertuš, J. Tomasi, Approximate evaluations of the electrostatic free energy and internal energy changes in solution processes. *Chem. Phys.* **65**, 239–245 (1982).
52. J. L. Pascual-ahuir, E. Silla, I. Tuñon, GEPOL: An improved description of molecular surfaces. III. A new algorithm for the computation of a solvent-excluding surface. *J. Comput. Chem.* **15**, 1127–1138 (1994).
53. H. Wang, G. Qu, J. Li, J. Ma, J. Guo, Y. Miao, J. Sun, Data mining of amine dehydrogenases for the synthesis of enantiopure amino alcohols. *Cat. Sci. Technol.* **10**, 5945–5952 (2020).
54. M. Rodenes, F. Gonell, S. Martín, A. Corma, I. Sorribes, Molecularly engineering defective basal planes in molybdenum sulfide for the direct synthesis of benzimidazoles by reductive coupling of dinitroarenes with aldehydes. *JACS Au* **2**, 601–612 (2022).
55. A. Vasu, M. Naresh, G. K. Sai, Y. D. Rohini, B. Murali, M. Ramulamma, A. Ramunaiduc, N. Narender, A heterogeneous catalytic strategy for facile production of benzimidazoles and quinoxalines from primary amines using the Al-MCM-41 Catalyst. *Green Chem.* **23**, 9439–9446 (2021).
56. L. Enders, D. S. Casadio, S. Aikonen, A. Lenarda, T. Wirtanen, T. Hu, S. Hietala, L. S. Ribeiro, M. R. Pereira, J. Helaja, Air oxidized activated carbon catalyst for aerobic oxidative aromatizations of N-heterocycles. *Cat. Sci. Technol.* **11**, 5962–5972 (2021).
57. T. Song, P. Ren, Z. Ma, J. Xiao, Y. Yang, Highly dispersed single-phase Ni2P nanoparticles on N, P-codoped porous carbon for efficient synthesis of N-heterocycles. *ACS Sustain. Chem. Eng.* **8**, 267–277 (2020).

Acknowledgments

Funding: This work was supported by the Program of National Natural Science Foundation of China (grant no. 22178170); the Jiangsu Province Natural Science Foundation for Distinguished Young Scholars (grant no. BK20190035); the National Key Research and Development Program of China (grant no. 2019YFD1101202); the Six Talent Peaks Project in Jiangsu Province (SWYY-045); the Jiangsu Province Natural Science Foundation for Youth (grant no. BK20200685); and the China Postdoctoral Science Foundation Funded Project (grant no. 2019 M660113). **Author contributions:** Z.T., X.Z., M.X., and Y.F. performed the experiments, analyzed the data, and participated in experiment design. W.Z. and M.L. commented on chemoenzymatic catalysis. X.W. provided a discussion on mechanism analysis. Z.T. and C.Z. prepared the manuscript. Z.T., H.Y., P.O., and C.Z. conceived and designed the experiments, supervised the work, and confirmed the manuscript. **Competing interests:** The authors declare that they have no competing interests. **Data and materials availability:** All data needed to evaluate the conclusions in the paper are present in the paper and/or the Supplementary Materials.

Submitted 26 May 2022
Accepted 25 July 2022
Published 7 September 2022
10.1126/sciadv.add1912